Anomalous and Solar Cosmic Ray Observations with the First Brazilian Scientific Microsatellite

Article · January 1995

13 authors, including:

Jim Adams
University of Alabama in Huntsville

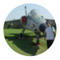

Inacio Martin
Instituto de Aeronáutica e Espaço

Thyrso Villela
National Institute for Space Research, Brazil

Allan J. Tylka
NASA

1995ICRC....4.1275T

Anomalous and Solar Cosmic Ray Observations with the First Brazilian Scientific Microsatellite

A. Turtelli, Jr.[1], T. Kohno[3], U. B. Jayanthi[2], J. H. Adams, Jr.[5],
I .M. Martin[1], T. Villela[2], A. Neri[2],
A. A. Gusev[1], G. I. Pugacheva[1], H. Kato[3],
K. Nagata[4], A. J. Tylka[5], P. R. Boberg[5,6]

[1] *University of Campinas (UNICAMP), Campinas, SP, Brazil*
[2] *Institute Nacional de Pesquisas Espaciais (INPE),*
S. J. Campos, SP, Brazil
[3] *The Institute of Physical and Chemical Research (RIKEN),*
Saitama, Japan
[4] *Tamagawa University, Machida, Tokyo, Japan*
[5] *Naval Research Laboratory, Washington DC, USA*
[6] *NRC Postdoctoral Research Associate*

Abstract

SACI 1, the first Brazillian scientific microsatellite[1], will be launched into a sun synchronous orbit (750 km altitude and 98° inclination) at the end of 1996. We plan to observe solar and anomalous ions with the ORCAS detector on SACI 1. In addition, ORCAS will measure ≈ 1 sec proton, helium, and electron fluxes in several energy bands.

1 Introduction

The ORCAS (Observações de Raios-Cosmicos Anomalos e Solares)[2] instrument is designed to measure the energetic ion fluxes in the magnetosphere, concentrating on studies of:

1. Anomalous cosmic rays (ACRs) in the Earth's magnetosphere. Recent low altitude experiments have determined two magnetospheric populations of anomalous cosmic rays: (1) predominantly singly-ionized ACRs[3], i.e. those above the geomagnetic cutoff, and (2) geomagnetically-trapped ACRs[4, 5], which become trapped after orbital electron stripping via atmospheric interactions[6]. Since SACI 1 will operate during the probable ACR maximum (solar minimum)[7], it is well suited for studying these populations, particularly the trapped ACRs. ORCAS measurements will assess the criterion for stable trapping[8, 9, 10, 11, 12] and the altitude dependence of trapped ACRs[13] beyond the Cosmos and SAMPEX observations.

2. Trapped light ions. Recent measurements[5, 14] have demonstrated a complex distribution of trapped helium ions in the inner magnetosphere. ORCAS will examine the origins and dynamics of both the stably and sporadically trapped helium fluxes recently observed by SAMPEX[5] and OHZORA[14].

3. Solar energetic particles. Using the Earth's magnetic field as a magnetic analyzer, the charge states of solar energetic particle (SEP) ions will be measured[15, 16]. If observations continue into the next solar maximum, the number of high energy, heavy ion events measured by ORCAS should far exceed previous samples[16], allowing analyses of event variability due both to SEP acceleration dynamics[16] and geomagnetic activity[17].

4. Trapped radiation dynamics. The recent measurements[18, 19, 20, 21, 22] by the CRRES, COSMOS, OHZORA, AKEBONO, and SAMPEX satellites revealed dramatic processes (injection and rapid penetration) contributing to the formation of trapped energetic p, e, and α populations in the slot region and inner belt.

5. The SAA. ORCAS will study possible connections between precipitating fluxes and aeronomical effects in the South Atlantic Anomaly region.

2 Design of the ORCAS telescope for SACI 1

Development of the First Brazillian Scientific Microsatellite (SACI 1) is now underway[1]. This satellite will be launched as a piggy-back on the CBERS remote sensing satellite. SACI 1 will contain 5 scientific instruments, will be spin stabilized (10 rpm), have a payload mass of $\sim$ 20 kg, total mass of $\sim$ 60 kg, 30 watts of experimental power, and design lifetime of 18 months.

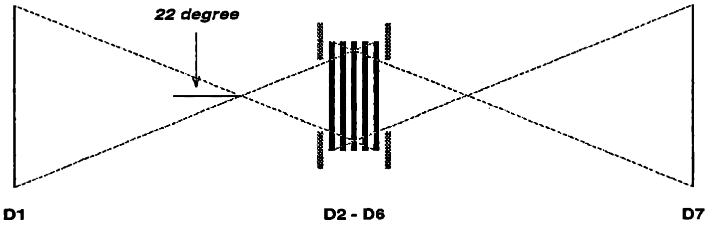

Figure 1: Schematic diagram of the telescope. D1 and D7 are ΔE detectors with sizes of $0.2 \times 48 \times 48 mm^3$. D2 - D6 are five energy detectors with effective sizes of $1 \times 28 \times 28 mm^3$. The bidirectional geometric factor is about $2.5 cm^2 \cdot sr$.

In order to maximize the detector acceptance and to economize the use of satellite resources, we plan to obtain elemental resolution over the largest possible energy range, geometry factor, and atomic numbers. Since the microsatellite is only about 40 cm wide, we maximized the geometry factor by designing a bidirectional telescope, as shown in Fig. 1. In order to maximize the energy acceptance and obtain elemental resolution, the telescope consists of silicon pin diode detectors, five 1.0 mm thick energy detectors and two 0.2 mm thick ΔE detectors. Each energy detector, D2 - D6, consists of two 0.5 mm thick sections with a 0.02 mm thick dead layer in each section. Simulated detector response curves for vertically incident helium and oxygen ions are showed in Fig. 2. By using the bank of discriminators shown in the electronic

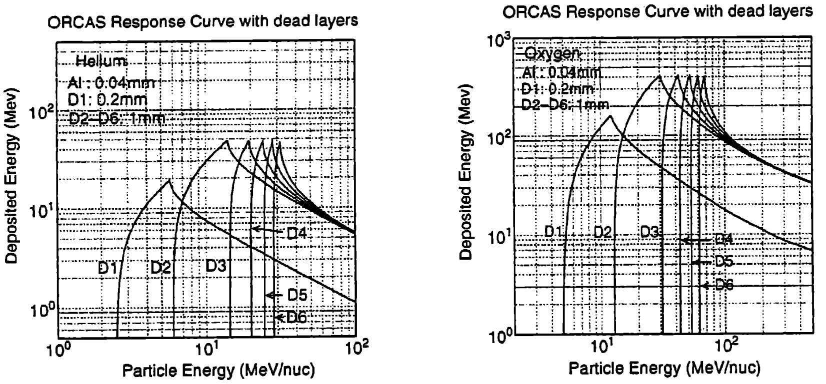

Figure 2: Simulated D1 to D6 detector responses for vertically incident helium (left) and for oxygen ions (right). The thin shielding and all dead layers are taken into account.

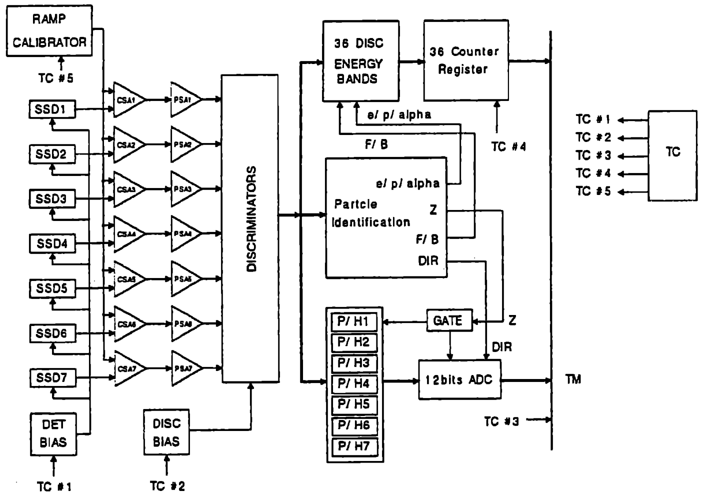

Figure 3: The electronic block diagram for the ORCAS telescope. The discriminators and priority encoder will separate electrons, protons and helium ions into several energy channels. Events judged as heavier than helium will be pulse height analyzed and all detectors' pulse heights will be telemetered to the ground.

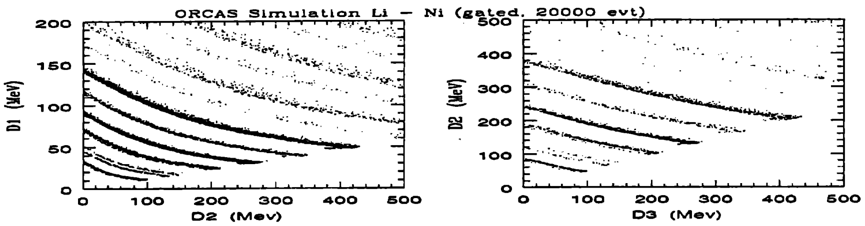

Figure 4: Simulated energy losses for Li to ≈ Ne (from full Li to Ni simulations) assuming GCR abundances for D1 vs. D2 (left) and D2 vs. D3 (right).

block diagram (Fig. 3), electron, proton and helium count rates in several energy channels will be recorded ≈ 8 times per spin period. An event judged as an element heavier than helium will be pulse height analyzed and all their data will be telemetered to the ground. Elemental observations are now tentatively planned from Li to Ne, with an energy acceptance of 12 to 70 MeV/nuc at oxygen.

3 Simulation of Heavy Ion Energy Losses

We performed a numerical simulation to check the telescope's ability to separate elements. We included the following items in this simulation: (1) isotropic event generation on D1, (2) coincidence between D1 and D2 is necessary for data recording, (3) energy loss, straggling, and detector dead layers, (4) signal fluctuation corresponding to a standard-deviation detector thickness nonuniformity of 0.5%, (5) elemental and isotopic abundance of galactic cosmic rays, and (6) power law energy spectrum of E^{-2}.

We show energy losses in the first two detector pair combinations in Fig. 4.

References

[1] Neri, A., Project Presentation at 1st Technical Scientific Workshop on SACI 1, INPE Sao Jose dos Campos, Brazil, March 8-10 1995.
[2] Turtelli, A., Jr., et al., ORCAS Propsal, Acadamia Braseileira Ciencias, (1994).
[3] Adams, J.H., Jr., et al., Ap.J., **377** (1991) L292.
[4] Grigorov, N.L., et al., GRL, **18** (1991) 1959.
[5] Cummings, J.R., et al., GRL, **20** (1993) 2003.
[6] Blake, J.B., & Friesen, L.M., Proc. 15th ICRC (Plovdiv), **2** (1977) 341.
[7] Mewaldt, R.A., et al., Proc. 23 ICRC (Calgary), **3** (1993) 404.
[8] Schulz, M., Blake, J.B., & McNab, C., unpublished manuscript.
[9] Ilyin, V.D., et al., Cos. Res., **31** (1993) 115.
[10] Tylka, A.J., Proc. 23rd ICRC (Calgary), **5** (1994) 465.
[11] Tylka, et al., Adv. Space Res., **17** (1995) (2)47.
[12] Selesnick, R.S., et al., JGR, (1995) in press.
[13] Tylka, A.J., et al., Proc. 24th ICRC (Rome), these proceedings.
[14] Kohno,T., et al., GRL, **22** (1995) 877.
[15] Boberg, P.R., et al., Proc. 23rd ICRC (Calgary), **3** (1993) 396.
[16] Tylka, A.J., et al., Ap.J. Lett., **444** (1995) L109.
[17] Boberg, P.R., et al., GRL, **22** (1995) 1133.
[18] Kohno, T., et al., Planet. Space Sci., **38** (1990) 483.
[19] Blake, J.B., et al., GRL, **19** (1992) 821.
[20] Baker, D.N., et al., GRL, **21** (1994) 409.
[21] Martin, I.M., et al., Rev. Bras. Geo., **13** (1995) 57.
[22] Gusev, A.A., et al., Planet. Sp. Sci., (1995) in press.